

Cite this: *Chem. Sci.*, 2018, 9, 4104

How does chiral self-sorting take place in the formation of homochiral Pd₆L₈ capsules consisting of cyclotrimeratrylene-based chiral tritopic ligands?†

Shumpei Kai,^a Tatsuo Kojima,^a Flora L. Thorp-Greenwood,^b Michael J. Hardie^b and Shuichi Hiraoka^{*a}

The chiral self-sorting process during the self-assembly of homochiral Pd₆L₈ capsules from cyclotrimeratrylene (CTV)-based chiral tritopic ligands (L) and PdPy₄^{*}(OTf)₂ (Py^{*}: 3-chloropyridine) was investigated by an NMR-based approach (QASAP: quantitative analysis of the self-assembly process). From the beginning to the formation of the Pd₆L₈Py₂^{*} immature capsules (ICs), enantiomeric ligands are distributed in the intermediates in a non-self-sorting manner, which leads to the isomers of heterochiral ICs over 99% yield. The mismatch of the chirality in the heterochiral ICs prevents intramolecular ligand exchanges in ICs to form the heterochiral capsules. The correction of the chirality in the heterochiral ICs (chiral self-sorting) takes place very slowly to finally lead to the homochiral capsules. The reason why the chiral self-sorting took place in the late stage of the self-assembly (after the formation of the heterochiral ICs) would be due to the relatively high flexibility of the CTV-based ligand.

Received 6th March 2018

Accepted 26th March 2018

DOI: 10.1039/c8sc01062e

rsc.li/chemical-science

Introduction

Chiral self-sorting is a phenomenon of chiral recognition where homochiral or heterochiral assemblies are favored over a statistical distribution under thermodynamic control arising from mutual discrimination between enantiomeric components.¹ Cyclotrimeratrylene (CTV) derivatives possessing two kinds of substituents alternately introduced on the rim of CTV have helical chirality.² Upon the complexation of a racemic mixture of the CTV-based tritopic ligand, **1**, with Pd(II) ions, homochiral octahedron-shaped Pd₆L₈ capsules are self-assembled through the homochiral self-sorting of enantiomeric ligands, **1^P** and **1^M** (Fig. 1).³ Which is favored, homochiral or heterochiral assemblies, is determined by relative thermodynamic stabilities of the diastereomeric isomers, but how chiral self-sorting takes place has been an unresolved question. For the understanding of the chiral self-sorting process, it is necessary to obtain information concerning intermediates that are transiently produced. To achieve this, a reliable method to investigate molecular self-assembly processes was recently developed by the authors (QASAP: quantitative analysis of

the self-assembly process).⁴ In most cases, most of the intermediates cannot be observed by spectroscopy, which has prevented us from investigating molecular self-assembly processes. On the other hand, QASAP enables us to obtain information about the intermediates as an average composition of all the intermediates by quantifying all the substrates and the products, so it is possible to reveal molecular self-assembly processes even if any intermediates are not observed. Here we report the chiral self-sorting process of homochiral Pd₆L₈ capsules assembled from Pd(II) ions (PdPy₄^{*}(OTf)₂, Py^{*} = 3-chloropyridine) and CTV-based chiral tritopic ligands, **1**, by QASAP (Fig. 1). The self-assembly takes place without chiral discrimination between the enantiomeric ligands until the formation of Pd₆L₈Py₂^{*} immature capsules (ICs). Most of the isomers of ICs are heterochiral species, which are kinetically trapped at 298 K, and their transformation into the heterochiral capsules is prevented. The correction of the chirality in the heterochiral ICs took place significantly slowly and with the aid of free **1** to lead to the homochiral ones, which are finally converted into the homochiral capsules by intramolecular ligand exchanges.

Results and discussion

Self-assembly of the Pd₆L₈ capsule from one-handed tritopic ligand and Pd(II) ions

Racemization of chiral CTV derivatives takes place by heating through the crown-to-crown flip of the CTV ring (*E*_{act} =

^aDepartment of Basic Science, Graduate School of Arts and Sciences, The University of Tokyo, 3-8-1 Komaba, Meguro-ku, Tokyo 153-8902, Japan. E-mail: chiraoka@mail.ecc.u-tokyo.ac.jp

^bSchool of Chemistry, University of Leeds, Woodhouse Lane, Leeds LS2 9JT, UK

† Electronic supplementary information (ESI) available: Experimental details, additional data, ¹H NMR spectra, ESI-TOF mass spectra and QASAP data. See DOI: 10.1039/c8sc01062e

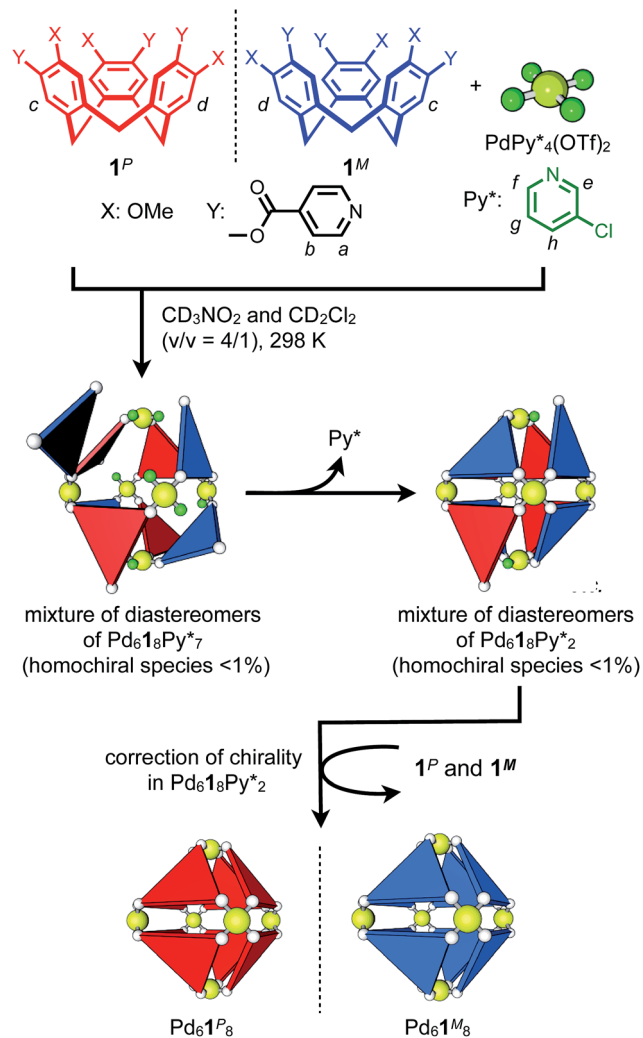


Fig. 1 Chiral self-sorting process of homochiral $\text{Pd}_6\text{18}$ capsules from a racemic mixture of **1** and $\text{PdPy}_4^*(\text{OTf})_2$ ($\text{Py}^* = 3\text{-chloropyridine}$) in CD_3NO_2 and CD_2Cl_2 ($v/v = 4/1$) at 298 K.

$26.5 \text{ kcal mol}^{-1}$),⁵ so the racemization of the tritopic ligands (**1**) in the intermediates is also involved in the chiral self-sorting when the self-assembly is carried out at high temperature. To investigate a strict chiral self-sorting process, avoiding the racemization of the chiral ligand, mild conditions under which the capsule formation takes place without heating are needed. Recently we found that the leaving ligands (X) on a $\text{Pd}(\text{II})$ ion source, $[\text{PdX}_4]^{2+}$, affect the coordination self-assembly process of a capsule⁶ and a cage.⁷ Compared to the generally employed $[\text{Pd}(\text{CH}_3\text{CN})_4]^{2+}$, $[\text{PdPy}_4^*]^{2+}$ ($\text{Py}^* = 3\text{-chloropyridine}$) tends to produce thermodynamically stable assembled structures much faster at room temperature, despite the coordination ability of Py^* being stronger than that of CH_3CN . Thus the self-assembly of the $\text{Pd}_6\text{18}$ capsule from one-handed **1**, which is indicated as **1**^{*} hereafter, and $\text{PdPy}_4^*(\text{OTf})_2$ in CD_3NO_2 and CD_2Cl_2 ($v/v = 4/1$) at 298 K was carried out and monitored by ^1H NMR spectroscopy (Fig. 2a). As expected, the self-assembly of the capsule from **1**^{*} smoothly took place at 298 K. On the other hand, when $\text{Pd}(\text{CH}_3\text{CN})_4(\text{OTf})_2$ was used as a metal source instead of

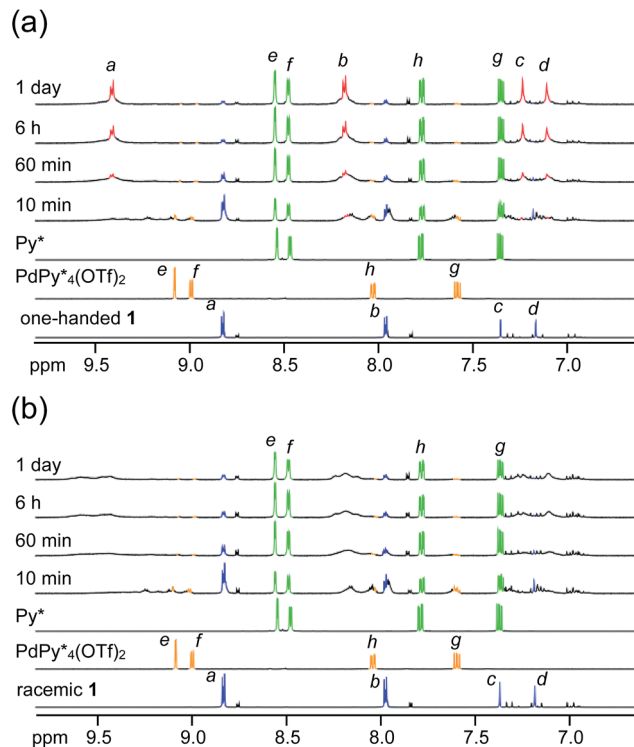


Fig. 2 Partial ^1H NMR spectra (500 MHz, aromatic region, CD_3NO_2 and CD_2Cl_2 ($v/v = 4/1$), 298 K) of the reaction mixture of the self-assembly of the homochiral $\text{Pd}_6\text{18}$ capsule(s) from $\text{PdPy}_4^*(\text{OTf})_2$ and (a) one-handed **1**, **1**^{*} ($[\text{1}^*]_0 = 2.2 \text{ mM}$) and (b) a racemic mixture of **1** ($[\text{1}]_0 = 2.2 \text{ mM}$). The lettering refers to that shown in Fig. 1.

$\text{PdPy}_4^*(\text{OTf})_2$, the signals assigned to the capsule were not observed (Fig. S1a†). A similar result was found even when the self-assembly was carried out in a strongly coordinative solvent, $\text{DMSO}-d_6$, at 298 K (Fig. S1b†).

QASAP for the self-assembly of the $\text{Pd}_6\text{18}$ capsule from one-handed tritopic ligands and $\text{Pd}(\text{II})$ ions

The self-assembly process of the capsule from **1**^{*} was analyzed by QASAP. The existence ratios of the substrates (**1**^{*} and $\text{PdPy}_4^*(\text{OTf})_2$), the products ($\text{Pd}_6\text{18}$ and Py^*), and all the intermediates (**Int**), whose ^1H NMR signals were not observed (Fig. 2a), are shown in Fig. 3a and b, S2a and Tables S1–S4.† One of the features of this self-assembly is that both the substrates remain until the end of the self-assembly. Every intermediate produced in the self-assembly is expressed as $\text{Pd}_{a1b}\text{Py}_c^*$, where a – c are positive integers or 0. As the information about the intermediates obtained by QASAP is the average composition of all the intermediates, $\text{Pd}_{(a)}\text{1}_{(b)}\text{Py}_{(c)}^*$, a further investigation was carried out by n – k analysis. The change in the intermediates is quantitatively analyzed by the time variation of two parameters, $\langle n \rangle$ and $\langle k \rangle$, which are derived from $\text{Pd}_{(a)}\text{1}_{(b)}\text{Py}_{(c)}^*$. The n value indicates the average number of $\text{Pd}(\text{II})$ ions binding to a single tritopic ligand ($\langle n \rangle = (4\langle a \rangle - \langle c \rangle) / \langle b \rangle$), while the $\langle k \rangle$ value indicates the composition ratio of the $\text{Pd}(\text{II})$ ion and the tritopic ligand ($\langle k \rangle = \langle a \rangle / \langle b \rangle$).⁴



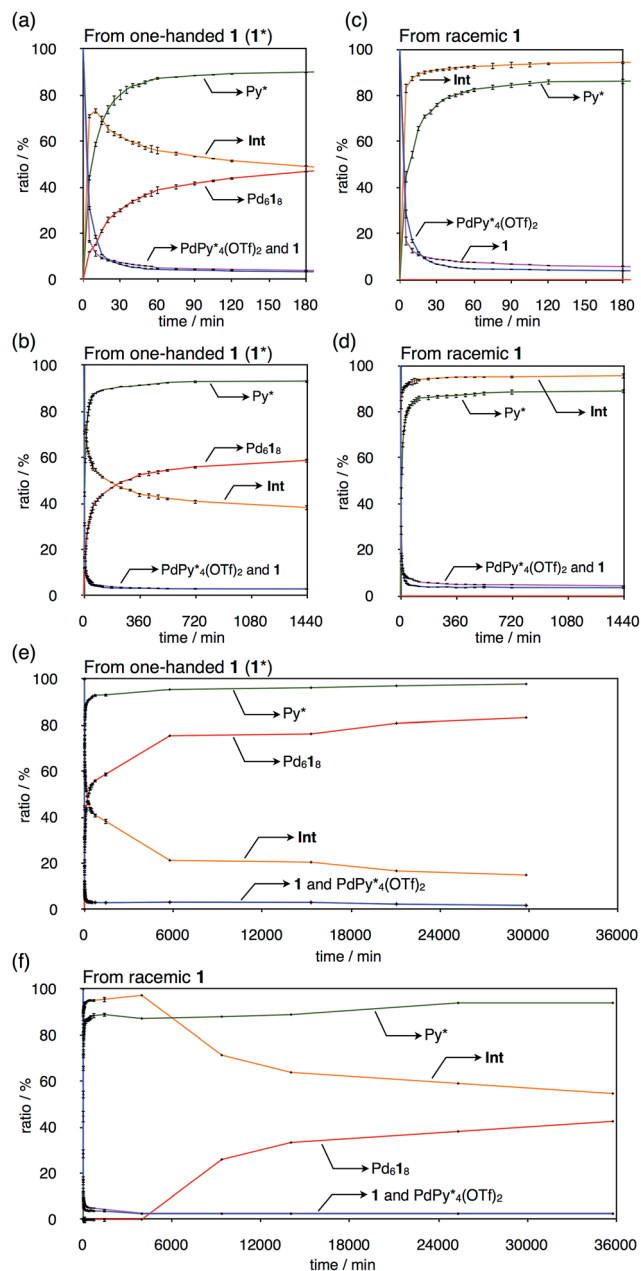


Fig. 3 Existence ratios of the substrates ($\text{PdPy}_4(\text{OTf})_2$ and $\mathbf{1}$), the products ($\text{Pd}_6\mathbf{L}_8$ and Py^*), and all the intermediates (Int) for the self-assembly of the homochiral $\text{Pd}_6\mathbf{L}_8$ capsule(s) from $\mathbf{1}$ and $\text{PdPy}_4(\text{OTf})_2$ in CD_3NO_2 and CD_2Cl_2 ($v/v = 4/1$) at 298 K. (a) From one-handed $\mathbf{1}$, $\mathbf{1}^*$ ($[\mathbf{1}^*]_0 = 2.2 \text{ mM}$) (from 0 to 180 min). (b) From one-handed $\mathbf{1}$, $\mathbf{1}^*$ ($[\mathbf{1}^*]_0 = 2.2 \text{ mM}$) (from 0 to 1 day). (c) From a racemic mixture of $\mathbf{1}$ ($[\mathbf{1}]_0 = 2.2 \text{ mM}$) (from 0 to 180 min). (d) From a racemic mixture of $\mathbf{1}$ ($[\mathbf{1}]_0 = 2.2 \text{ mM}$) (from 0 to 1440 min). (e) From a racemic mixture of $\mathbf{1}$ ($[\mathbf{1}]_0 = 2.2 \text{ mM}$) (from 0 to 30 000 min). (f) From a racemic mixture of $\mathbf{1}$ ($[\mathbf{1}]_0 = 2.2 \text{ mM}$) (from 0 to 36 000 min). Blue, magenta, red, green, and orange lines indicate $\text{PdPy}_4(\text{OTf})_2$, $\mathbf{1}$, $\text{Pd}_6\mathbf{L}_8$, Py^* , and Int, respectively.

The change in the $\langle n \rangle$ and $\langle k \rangle$ values with time is shown in Fig. 4a and b. At 5 min, the $(\langle n \rangle, \langle k \rangle)$ value was plotted around the (n, k) values of species containing fewer components than the capsule and then both $\langle n \rangle$ and $\langle k \rangle$ values increased with time to reach around (6, 8, 7) and (6, 8, 6) at 20 min ((a, b, c)

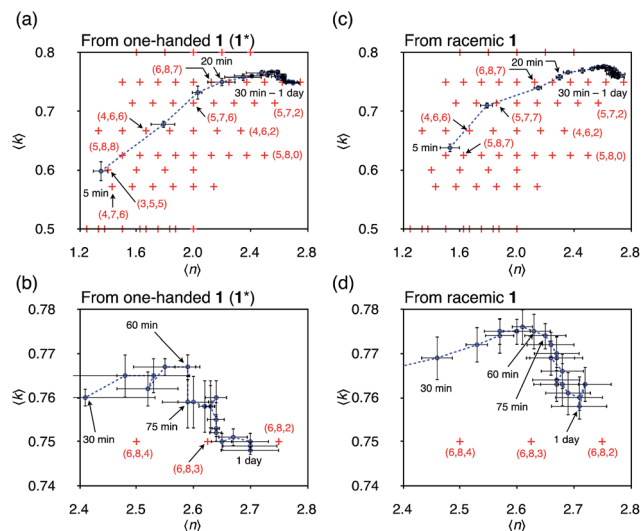


Fig. 4 $n-k$ plots for the self-assembly of the homochiral $\text{Pd}_6\mathbf{L}_8$ capsule(s) from $\mathbf{1}$ and $\text{PdPy}_4(\text{OTf})_2$ in CD_3NO_2 and CD_2Cl_2 ($v/v = 4/1$) at 298 K. (a and b) From one-handed $\mathbf{1}$, $\mathbf{1}^*$ ($[\mathbf{1}^*]_0 = 2.2 \text{ mM}$). (c and d) From a racemic mixture of $\mathbf{1}$ ($[\mathbf{1}]_0 = 2.2 \text{ mM}$). Red crosshairs indicate the (n, k) value of $\text{Pd}_a\mathbf{L}_b\text{Py}_c^*$ ($a \leq 6$ and $b \leq 8$). (a, b, c) indicates $\text{Pd}_a\mathbf{L}_b\text{Py}_c^*$.

indicates $\text{Pd}_a\mathbf{L}_b\text{Py}_c^*$). The increase in the $\langle n \rangle$ and $\langle k \rangle$ values reflects the incorporation of free ligands ($\mathbf{1}^*$) and $\text{Pd}(\text{II})$ ions with a release of Py^* molecules through intra- and/or intermolecular ligand exchanges. After 20 min, the $\langle n \rangle$ value increased with no significant change in the $\langle k \rangle$ value and the $(\langle n \rangle, \langle k \rangle)$ value finally converged to the (n, k) values of $\text{Pd}_6\mathbf{L}_8\text{Py}_2^*$ and $\text{Pd}_6\mathbf{L}_8\text{Py}_3^*$ (Fig. 4b). This result indicates that the intramolecular ligand exchanges in $\text{Pd}_6\mathbf{L}_8\text{Py}_7^*$ took place after 20 min and led to a mixture of $\text{Pd}_6\mathbf{L}_8\text{Py}_2^*$ and $\text{Pd}_6\mathbf{L}_8\text{Py}_3^*$ and that the further intramolecular ligand exchanges within them became slow. A similar trend that the intramolecular ligand exchange in the late stage of the self-assembly becomes the rate-determining step was found in the self-assembly of $\text{Pd}_6\mathbf{L}_8$ capsules from hexaphenylbenzene-based tritopic ligands⁸ and of a $\text{Pd}_2\mathbf{L}_4$ cage from ditopic ligands possessing two pyridyl groups connected to a benzene ring through an ethynyl spacer.⁷

Monitoring of the self-assembly of the $\text{Pd}_6\mathbf{L}_8$ capsule from one-handed tritopic ligands and $\text{Pd}(\text{II})$ ions by mass spectrometry

The self-assembly of the capsule from $\mathbf{1}^*$ and $\text{PdPy}_4(\text{OTf})_2$ was monitored by ESI-TOF mass spectrometry (Fig. S3†) and the mainly observed species are summarized in Table 1. The species that contain more components than the capsule were not found. In most species (indicated by underlining in Table 1), $\text{Pd}(\text{II})$ ion(s) is/are coordinately unsaturated. As no liberation of Py^* from $\text{PdPy}_4(\text{OTf})_2$ occurred in CD_3NO_2 and CD_2Cl_2 ($v/v = 4/1$) at 298 K (confirmed by ^1H NMR), these coordinately unsaturated species should be produced during the ionization process,⁶ which suggests that the intermediates should have more Py^* molecules than were detected by mass spectrometry. With this in mind, the signals for $\text{Pd}_6\mathbf{L}_8\text{Py}_0^*$ ($= (6, 8, 0)$) should derive from not only the capsule but also $\text{Pd}_6\mathbf{L}_8\text{Py}_c^*$ ($c > 0$). Thus

Table 1 Time variation of the $\text{Pd}_6\text{1}_8^*\text{Py}_c^*$ designated (a, b, c) species detected by ESI-TOF mass spectrometry for the self-assembly of the $\text{Pd}_6\text{1}_8^*(\text{OTf})_{12}$ capsule from $\text{PdPy}_4^*(\text{OTf})_2$ and **1*** ($[\text{1}^*] = 2.2 \text{ mM}$) in CD_3NO_2 and CD_2Cl_2 ($v/v = 4/1$) at 298 K

5 min	10 min	30 min	60 min	120 min	180 min	360 min
<u>(1, 1, 0)</u> ^a	<u>(1, 1, 0)</u>	<u>(1, 1, 0)</u>	<u>(1, 1, 0)</u>	<u>(1, 1, 0)</u>	<u>(1, 1, 0)</u>	<u>(1, 1, 0)</u>
<u>(1, 1, 2)</u>	<u>(1, 1, 2)</u>	<u>(1, 1, 2)</u>	<u>(1, 1, 2)</u>	<u>(1, 1, 2)</u>		
<u>(1, 2, 0)</u>	<u>(1, 2, 0)</u>	<u>(1, 2, 0)</u>	<u>(1, 2, 0)</u>	<u>(1, 2, 0)</u>	<u>(1, 2, 0)</u>	<u>(1, 2, 0)</u>
<u>(2, 2, 0)</u>	<u>(2, 2, 0)</u>	<u>(2, 2, 0)</u>	<u>(2, 2, 0)</u>	<u>(2, 2, 0)</u>	<u>(2, 2, 0)</u>	<u>(2, 2, 0)</u>
<u>(2, 2, 2)</u>						
<u>(2, 3, 0)</u>	<u>(2, 3, 0)</u>	<u>(2, 3, 0)</u>	<u>(2, 3, 0)</u>	<u>(2, 3, 0)</u>	<u>(2, 3, 0)</u>	<u>(2, 3, 0)</u>
<u>(3, 8, 3)</u>	<u>(3, 8, 3)</u>	<u>(3, 8, 3)</u>	<u>(3, 8, 3)</u>	<u>(3, 8, 3)</u>	<u>(3, 8, 3)</u>	<u>(3, 8, 3)</u>
<u>(6, 8, 0)</u>	<u>(6, 8, 0)</u>	<u>(6, 8, 0)</u>	<u>(6, 8, 0)</u>	<u>(6, 8, 0)</u>	<u>(6, 8, 0)</u>	<u>(6, 8, 0)</u>

^a Underlines indicate the species whose Pd(II) ion center(s) is/are coordinately unsaturated.

$\text{Pd}_6\text{1}_8^*\text{Py}_c^*$ ($c = 2-7$), whose existence is proposed by $n-k$ analysis, should be detected as $\text{Pd}_6\text{1}_8^*\text{Py}_0^*$ by mass spectrometry. On the other hand, $\text{Pd}_3\text{1}_8^*\text{Py}_3^*$ ($= (3, 8, 3)$) has more Py^* molecules than the maximum number of 2, which would be generated by the addition of Py^* to $\text{Pd}_3\text{1}_8^*\text{Py}_c^*$ ($c = 0-2$) during the ionization.

Chiral self-sorting process in the formation of the $\text{Pd}_6\text{1}_8$ capsule revealed by QASAP

The self-assembly of the capsule from a racemic mixture of **1** under the same conditions was monitored by ^1H NMR spectroscopy (Fig. 2b). Though the consumption of the substrates and the release of Py^* were observed, no signals for the homochiral capsule were found until 1 day and the signals for the homochiral capsules appeared after 1 week (Fig. 2b and 3f). The change in the existence ratios of the substrates and Py^* in the beginning of the self-assembly from a racemic mixture of **1** is similar to that from **1*** but the formation of the homochiral capsules was significantly retarded (Fig. 3e and f). This result indicates that the heterochiral species that are difficult to convert into homochiral ones were predominantly produced. The change in the $\langle n \rangle$ and $\langle k \rangle$ values with time for a racemic mixture of **1** is similar to that for **1*** (Fig. 4c and d). Monitoring the self-assembly by ESI-TOF mass spectrometry also detected the same species as in the self-assembly from **1*** (Fig. S4†). These results indicate that the self-assembly of the capsule from a racemic mixture of **1** takes place as follows. In the beginning of the self-assembly, small species are produced and then grow by the incorporation of the substrates to lead to the heterochiral isomers of $\text{Pd}_6\text{1}_8\text{Py}_c^*$ ($c = 6$ and 7), which are converted into the heterochiral $\text{Pd}_6\text{1}_8\text{Py}_2^*$ immature capsules (ICs) by intramolecular ligand exchanges. As the capsule formation was not observed until 1 day, $\text{Pd}_6\text{1}_8\text{Py}_2^*$ should be kinetically trapped. The heterochiral $\text{Pd}_6\text{1}_8$ capsules have many diastereomeric isomers with different composition ratios of the enantiomers of **1** and with different arrangements of the enantiomers on the faces of the octahedron, which should cause many chemically inequivalent ^1H NMR signals. Thus there remains the possibility that the signals for the heterochiral capsules are included in significant broad signals (Fig. 2b). However, the formation of the heterochiral capsules would be

excluded by the fact that in the case of the self-assembly from a racemic mixture of **1** the release ratio of Py^* is lower than that from **1*** (Fig. 3), and that the $\langle n \rangle$, $\langle k \rangle$ values in both cases after convergence are similar to each other (Fig. 4). If a non-negligible amount of the heterochiral capsules is included in **Int**, higher $\langle n \rangle$ values for a racemic mixture of **1** than that for **1*** are expected. The difficulty in the intramolecular ligand exchanges in the heterochiral ICs is due to the mismatch between the enantiomers of **1**, which would cause higher energy barriers of the intramolecular ligand exchanges in the heterochiral ICs.

If the self-assembly of the capsule takes place under the statistical situation, the formation ratio of the homochiral capsules, which are composed of eight ligands with the same chirality (SSSSSSSS and RRRRRRRR), is 0.78%. The statistical formation of the mixture of the ICs is thus consistent with no observation of the signals for the homochiral capsules until 1 day and the formation of the mixture of the ICs should occur in a statistical manner if there is no preference of some of the heterochiral species. The statistical self-assembly is reasonable considering the high flexibility of the pyridyl groups connected to the rim of CTV by ester bonds. The signals for the homochiral capsules appeared after 1 week and the yield of the homochiral capsules was as high as 40% at 25 days (Fig. 3f), which indicates that the homochiral self-sorting took place after 1 day. Considering the associative ligand exchange mechanism on Pd(II) centers, the free tritopic ligands **1** remaining in the reaction mixture would trigger biasing the chirality of the heterochiral ICs toward homochirality.⁹

Conclusions

In conclusion, the chiral self-sorting process in the formation of homochiral capsules from a racemic mixture of CTV-based tritopic ligands, **1**^P and **1**^M, and $\text{PdPy}_4^*(\text{OTf})_2$ was revealed by QASAP under mild conditions for which the racemization of **1** does not take place. As far as the composition ratio of the components in the intermediates is concerned, the intermediates produced in the self-assembly from one-handed **1** (**1***) and that from a racemic mixture of **1** are quite similar. It was found that no chiral self-sorting took place until the formation of a diastereomeric and structural mixture of the $\text{Pd}_6\text{1}_8\text{Py}_2^*$ immature capsules (ICs), whose intramolecular ligand exchanges were prevented by the mismatch of the chirality between the chiral ligands in the heterochiral ICs and that the homochiral self-sorting took place by the correction of the chirality through the rearrangement of the components in the heterochiral ICs. Although the homochiral capsules are the most stable under thermodynamic control, significantly low or no chiral self-sorting occurred until the late stage of the self-assembly, which is because of the high flexibility of the pyridyl groups connected to the rim of CTV by ester bonds.

Conflicts of interest

There are no conflicts to declare.



Acknowledgements

This research was supported by JSPS Grants-in-Aid for Scientific Research on Innovative Areas “Dynamical Ordering of Biomolecular Systems for Creation of Integrated Functions” (25102001 and 25102005), The Asahi Glass Foundation, and the Leverhulme Trust (RPG-2014-148).

References

- (a) H. Jędrzejewska and A. Szumna, *Chem. Rev.*, 2017, **117**, 4863–4899; (b) L.-J. Chen, H.-B. Yang and M. Shionoya, *Chem. Soc. Rev.*, 2017, **46**, 2555–2576; (c) M. Liu, L. Zhang and T. Wang, *Chem. Rev.*, 2015, **115**, 7304–7397.
- (a) J. Canceill, A. Collet, J. Gabard, G. Gottarelli and G. P. Spada, *J. Am. Chem. Soc.*, 1985, **107**, 1299–1308; (b) J. Canceill, A. Collet and G. Gottarelli, *J. Am. Chem. Soc.*, 1984, **106**, 5997–6003; (c) A. Collet and G. Gottarelli, *J. Am. Chem. Soc.*, 1981, **103**, 204–205; (d) A. Collet and J. Jacques, *Tetrahedron Lett.*, 1978, **19**, 1265–1268.
- (a) T. K. Ronson, J. Fisher, L. P. Harding and M. J. Hardie, *Angew. Chem., Int. Ed.*, 2007, **46**, 9086–9088; (b) T. K. Ronson, C. Carruthers, J. Fisher, T. Brotin, L. P. Harding, P. J. Rizkal-lah and M. J. Hardie, *Inorg. Chem.*, 2010, **49**, 675–685; (c) J. J. Henkelis, J. Fisher, S. L. Warriner and M. J. Hardie, *Chem.–Eur. J.*, 2014, **20**, 4117–4125; (d) N. J. Cookson, J. J. Henkelis, R. J. Ansell, C. W. G. Fishwick, M. J. Hardie and J. Fisher, *Dalton Trans.*, 2014, **43**, 5657–5661.
- (a) S. Hiraoka, *Chem. Rec.*, 2015, **15**, 1144–1147; (b) A. Baba, T. Kojima and S. Hiraoka, *J. Am. Chem. Soc.*, 2015, **137**, 7664–7667.
- A. Collet and J. Gabard, *J. Org. Chem.*, 1980, **45**, 5400–5401.
- S. Kai, Y. Sakuma, T. Mashiko, T. Kojima, M. Tachikawa and S. Hiraoka, *Inorg. Chem.*, 2017, **56**, 12652–12663.
- S. Kai, V. Marti-Centelles, Y. Sakuma, T. Mashiko, T. Kojima, U. Nagashima, M. Tachikawa, P. J. Lusby and S. Hiraoka, *Chem.–Eur. J.*, 2018, **24**, 663–671.
- Y. Tsujimoto, T. Kojima and S. Hiraoka, *Chem. Sci.*, 2014, **5**, 4167–4172.
- (a) M. L. Tobe and J. Burgess, *Inorganic Reaction Mechanisms*, Longman, London, UK, 1999; (b) F. Basolo and R. G. Pearson, *Mechanisms of Inorganic Reactions: A Study of Metal Complexes in Solution*, John Wiley, and Sons, Inc., New York, 1967; (c) J. Cooper and T. A. Ziegler, *Inorg. Chem.*, 2002, **41**, 6614–6622.

